Research in Pharmaceutical Sciences, August 2025; 20(4): 485-497
Received: 27-8-2023
Peer Reviewed: 14-10-2023
Revised: 05-10-2024
Accepted: 11-11-2024
Published: 25-08-2025

School of Pharmacy & Pharmaceutical Sciences
Isfahan University of Medical Sciences

Original Article

Gold nanoparticles from *Artemisia absinthium*, *Morus nigra*, and *Peganum harmala*: biosynthesis, characterization, and their biological evaluations against cancer cells

Hojjat Sadeghi-Aliabadi[1], Mina Mirian[2,*], Arefeh Banizaman[1,3], Mahbobeh Rezazadeh[3], Fahimeh Rahimi[3], Soheila Sepahi[3,4], and Mahsa Sadeghi-Aliabadi[3,5]

[1]*Department of Medicinal Chemistry, School of Pharmacy and Pharmaceutical Sciences, Isfahan University of Medical Sciences, Isfahan, I.R. Iran.*
[2]*Department of Pharmaceutical Biotechnology, School of Pharmacy and Pharmaceutical Sciences, Isfahan University of Medical Sciences, Isfahan, I.R. Iran.*
[3]*Department of Pharmaceutics, School of Pharmacy and Pharmaceutical Sciences, Isfahan University of Medical Sciences, Isfahan, I.R. Iran.*
[4]*Food and Drug Organization, Isfahan University of Medical Sciences, Isfahan, I.R. Iran.*
[5]*Department of Medical Genetics, Islamic Azad University of Tehran Medical Sciences, Tehran, I.R. Iran.*

Abstract

Background and purpose: Metallic nanoparticles (NPs) can be applied in various biomedical fields, such as antibacterial and anti-cancer agents. Synthesizing metallic NPs by green chemistry procedures makes them eco-friendly and easier to prepare. This study aimed to develop 3 different gold (Au) NPs, using plant extracts including *Artemisia absinthium* (AA) aerial parts, *Morus nigra* (MN) fruits, and *Peganum harmala* (PH) seeds.

Experimental approach: Green AuNPs were synthesized by mixing plant extracts and $HAuCl_4.3H_2O$ and heating the mixture at 60 °C. Cytotoxic activity of synthesized AuNPs was evaluated using the MTT assay, followed by flow cytometry to assess its mechanism. Synthesis of plant AuNPs was confirmed by relevant color change, DLS, Zeta potential, and were characterized by a relevant surface plasmon resonance peak for AuNPs between 500 to 600 nm.

Findings/Results: AA-AuNPs, MN-AuNPs, and PH-AuNPs were cytotoxic against cancer cell lines in a dose-dependent manner. Results also revealed that PH-AuNPs were the most potent NPs (IC_{50} values of 7.7, 16.7, 30, and 40 µg/mL against HeLa, HT-29, OVCAR3 and MCF-7 cell lines, respectively). HeLa cells were the most sensitive cell line toward all tested NPs, significantly. Flow cytometry results confirmed that the cytotoxic effects of AuNPs were mediated through apoptosis induction.

Conclusion and implications: Using plants to formulate metallic NPs is inexpensive, easily accessible, and renewable. Additionally, due to their considerable cytotoxicity, their applications as a cancer treatment option is a promising approach that warrants further investigation. Thus, the rapidly synthesized AuNPs can play a role in nanotechnology and biomedical applications.

Keywords: *Artemisia absinthium*; Cytotoxicity; *Morus nigra*; Nanoparticles; *Peganum harmala.*

INTRODUCTION

Synthesis of metallic nanoparticles (NPs) by green chemistry procedures has been recently considered by scientists because of their eco-friendliness, easy preparation, and various applications (1,2). Different morphologies of prepared metallic compounds in nano-size offer an interesting approach to diffusion and interaction with target molecules (3).

Access this article online

Website: http://rps.mui.ac.ir

DOI: 10.4103/RPS.RPS_159_23

*Corresponding author: M. Mirian
Email: mina.mirian@pharm.mui.ac.ir
Tel: +98-3137927057, Fax: +98-3136680011

Among noble metals, using gold (Au) and silver (Ag) for the preparation of NPs is more common because they are more applicable and compatible with biological systems. For instance, AgNPs have been most widely applied as antimicrobial agents, whereas AuNPs have been utilized in the detection and treatment of cancers (4-6). It has been shown that AuNPs can enhance the quality of cancer treatment through increased permeability and maintenance of therapeutic agents in cancerous cells (7). In addition, AuNPs can be applied in photodynamic therapy because they absorb visible light and emit wavelengths with high energy toward the target tissue precisely and efficiently (8).

Nowadays, the most used and conventional method for the preparation of NPs is the chemical approach, followed by physical and biological procedures. Making NPs by chemical synthesis results in lower toxicity in the case of Au and/or equal toxicity in the case of Ag compared to bulk chemicals (3,9). The disadvantages of chemical-based synthesis of NPs, when considered for cellular applications, are their toxicity toward cells because they release chemicals gradually. The toxic effects could be reduced by the development and use of effective alternatives, such as NPs produced with the aid of plant extracts.

Plant-based active biological ingredients with antioxidant properties, such as phenolic compounds, terpenoids, and alkaloids, serve as both reducing and capping agents for NPs. Therefore, they are considered biomedical effective compounds (10-12).

Peganum harmala (PH) L. is a member of the family Zygophyllaceae, commonly known as Syrian rue in the world and Esfand in Iran, and grows in the middle parts of Iran. PH composition has been studied previously. Its ripe fruit (3.12%) and flower (3.27%) contain alkaloids, including harmine, peganine, and harmaline. PH seed essential oil composition consists of 2,3-dimethyl benzofuran, cis-linalool oxide, [2E]-decenal, 4aα,7β,7aα-nepetalactone, 3-oxo-p-menth-1-en-7-al and trans-β-terpineol (13,14). Its seeds are rich in carbolin alkaloids with a wide spectrum of pharmacological actions, including antispasmodic, antipyretic, analgesic, and anticancer activities (15). Esfand has been used in a pharmaceutical product called Spinal-Z (Darupakhsh Company), which has cytotoxic, anti-inflammatory, analgesic, anti-bacterial, and anti-viral effects and is used for the treatment of non-metastatic gastro-esophageal cancers (16).

The essential oil and extracts of *Artemisia absinthium* (AA) L. (Asteraceae), commonly known as wormwood in the world and Afsantin in Iran, contain compounds with antioxidant and antibacterial properties. Iranian wormwood essential oil is characterized by the predominance of β-pinene and β-thujone (17). The chemical structure of AA showed that it contains caryophyllene oxide (25.3%), p-cymene (16.8%), 1,8-cineole (8.9%), and (Z)-lanceol acetate (7.3%) (18). In addition, it has been reported that the extract of the AA aerial part induced anti-proliferative effects on human breast cancer cells (19).

Morus nigra (MN) L. commonly known as black mulberry, named shahtoot (King of mulberry), native to Iran, belongs to the family of Moraceae. It has long been cultivated for its edible fruit. Black mulberry trees are thought to have originated in the mountainous areas of Mesopotamia and Persia and are now introduced from Iran to most Middle Eastern countries. This deep-colored fruit contains riboflavin (vitamin B_2), niacin (vitamin B_3), and ascorbic acid (vitamin C). It is also rich in phenolic, flavonoid, and alkaloid contents (20-22).

The present study used the extracts of AA aerial parts, MN fruits, and PH seeds in the biosynthesis and characterization of Au-NPs against cancer cells. Some studies have used the plants in the synthesis of Au-NPs for their antibacterial effects (23,24). However, to the best of our knowledge, they have not previously been used for their cytotoxic effects against cancer cells. The objective of this study was to develop an eco-friendly, simple, cost-effective, and single-step method for the synthesis of 3 different AuNPs as anti-cancer agents, using plant extracts including AA aerial parts, MN fruits, and PH seeds.

MATERIALS AND METHODS

Plant extract preparation

AA aerial parts, MN fruits, and PH seeds were the medicinal plant parts used in the studies. The plants were characterized by the Department of Pharmacognosy, School of Pharmacy and Pharmaceutical Sciences, Isfahan University of Medical Sciences (Isfahan, Iran). Voucher specimens were made and deposited in the Herbarium of the School of Pharmacy and Pharmaceutical Sciences (Isfahan, Iran). Voucher numbers were 2310, 2519, and 1381 for PH, MN, and AA, respectively. Powdered plant materials (10 g) were extracted in 200 mL of deionized water by the maceration technique (25). The suspended plant material was initially heated at 60 °C for 10 min to avoid any possible degradation of the active biomolecules. The suspension was then stirred for 1 h at room temperature (24 °C). The extracted biomass was then centrifuged at 5000 rpm for 5 min to remove the bulk plant material. Finally, the obtained supernatant was filtered through Whatman No.1 filter paper. This filtered extract was directly used for the synthesis of NPs.

Synthesis of AuNPs

To synthesize AuNPs, the various volumes of the plant extracts (0.5-4 mL) were mixed separately with 10 mL of gold salt ($HAuCl_4.3H_2O$) solutions (1-4 mM). The reaction mixture was heated in a water bath at 60 °C until the reaction was completed. Synthesis progress was followed by visual observation of the color changed from yellow to deep purple within a few min (26). The synthesis mechanism of NPs has been explained previously (27).

Synthesis optimization of NPs

Various parameters that affect the synthesis of NPs were optimized to achieve the best final product. A fractional design (with 4 factors and 3 levels) was developed to explore the optimum level of the variables. Four independent variables, including the volume of extract (0.5-4 mL), $HAuCl_4.3H_2O$ concentrations (1-4 mM), pH (4-8), and reaction time (10-100 min) were studied at 3 different levels. The coded and actual values of the variables for MN, AA, and PH extracts were given in Tables S1-S3. Aliquots obtained from the reaction mixture were scanned at wavelengths between 350 to 750 nm. Optimized formulations were selected for toxicity evaluation by 3-[4,5-dimethylthiazol-2yl]-2,5 2,5-diphenyl tetrazolium bromide (MTT) assay, followed by flow cytometry against MCF-7, HT-29, OVCAR-3, and HeLa cells.

Structural features of plant-AuNPs

Plant-AuNPs were visualized by color changing, and absorbance spectra were detected by ultraviolet-visible (UV-Vis) spectrophotometer (Lambda 25, PerkinElmer, USA) between 350-750 nm wavelength ranges. The powder obtained from freeze-dried plant-AuNPs was further subjected to different analyses to confirm the anticipated NPs formation. A field emission scanning electron microscope (FESEM, TeScan-Mira III, Czech Republic) was used to monitor the shape of the synthesized plant-AuNPs. Hydrodynamic size distribution and zeta potential (ZP) of plant-AuNPs were measured by dynamic light scattering (DLS; Malvern Zeta-seizer, ZEN-3600, United Kingdom). Finally, Fourier-transform infrared (FT-IR) spectroscopy (FT/IR-6300, JASCO, Japan) was used to analyze the functional groups involved in the formation of plants-AuNPs.

Biological evaluation of plant-AuNPs

MCF-7, HT-29, OVCAR3, and HeLa cell lines derived from breast, colon, ovarian, and cervical cancers, respectively, were purchased from the Pasteur Institute (Tehran, Iran). All cell lines were grown in RPMI1640 (Bio-Idea, Iran) except for HT-29, which was cultured in Dulbecco's modified eagle's medium (DMEM) high glucose (Bio-Idea, Iran) supplemented with 1% essential amino acid (Gibco, USA), 1% antibiotics (5000 IU of penicillin and 50 µg/mL of streptomycin, Gibco, USA), and 10% fetal bovine serum (FBS) (Bio-Idea, Iran). Cells were maintained in a humidified incubator with 5% CO_2 at 37 °C.

MTT assay

The cytotoxic activity of the plant-AuNPs was analyzed by MTT assay. Briefly, cells were implanted in 96-well culture plates (5×10^4 cells/mL) and allowed to attach for 24 h, then treated with different concentrations (5, 10, 15, 20, 25, 30, 40, 80, and 160 µg/mL) of synthesized NPs, followed by a further 48 h incubation. After that, 20 µL of MTT solution

(5 mg/mL) was added to each well and incubated for 3 h. To dissolve the formed purple formazan crystals, 150 µL of media was replaced with dimethyl sulfoxide (DMSO), and the absorbance of each well was determined at 570 nm using a multi-well ELISA plate reader (Elx808, BioTech, USA) (28,29). Results were expressed as the percent of cell survival using the following equation:

$$Cell\ cervival\ (\%) = \frac{Ab_{treated\ sample} - Ab_{blank}}{Ab_{negative\ control} - Ab_{blank}} \times 100$$

where, Ab was put instead of the absorbance mean.

Flow cytometry assay

To evaluate the cell death mechanism induced by plant-AuNPs, an apoptosis assay was performed by flow cytometer (BD FACSCalibur, BD Biosciences, USA) based on the manufacturer's protocol using fluorescein isothiocyanate (FITC) Annexin V-propidium iodide (PI) staining kit (BioLegend, USA). In this regard, MCF-7, HT-29, OVCAR3, and HeLa cells were seeded in 12-well plates and then separately treated for 24 h at an IC_{50} concentration of the plant-AuNPs. Briefly, cells were washed twice with phosphate-buffered saline (PBS), and 100 µL of cell suspension (5×10^5 cells/mL) was transferred to the test tube, followed by adding 5 µL of FITC Annexin V solution and incubating for 15 min at room temperature. Then, the cells were washed with 400 µL of binding buffer. Finally, 5 µL of PI solution was added to the cells and subjected to flow cytometry. CellQuest Pro software (version 5.1, BD Biosciences, USA) was used for the interpretation of flow cytometry results.

Supplementary materials

The supplementary materials for this article can be found online at: https://github.com/Mirian1361/supplementary-materials.

Statistical analysis

Cell toxicity data were expressed as the mean ± standard deviation (SD). Microsoft SPSS 21 software was used to analyze data using one-way ANOVA, followed by LSD post-hoc. *P*-values < 0.05 were considered statistically significant.

RESULTS

Characteristics of extracts

To produce NPs, the plant extracts were mixed with the HAuCl4.3H2O solution at room temperature. The process of biosynthesis of plant-AuNPs was monitored by changes in the color during the reaction. Initially, when reducing agents (plant extracts) were added to the aqueous solution of $HAuCl_4.3H_2O$, the solution completely changed from yellow to a deep purple color within minutes.

Particle size and ZP of NPs

Particle size (PS), polydispersity index (PDI), and ZP of the examined formulation for each extract and the effect of different variables on the characteristics of NPs are shown in Tables S1-S3. For MN-AuNPs, PS was significantly increased with an increase in the amount of extract, pH, and reaction time. An increase in Au concentration from 1 mM to 2 mM decreased PS, while an increase to concentrations higher than 2 mM enhanced it. As for ZP, it was decreased by the elevation of the extract and increased by an increase in the concentration of Au. The time and pH values did not show significant effects on ZP. PDI for MN-AuNPs ranged from 0.4 to 0.6 and was increased by increasing in amount of extract and the concentration of Au (Table 1). The characteristics of AA-AuNPs, including PS, ZP, and PDI, were found to be very similar to the characterization of MN-AuNPs (Table 1). As for PH-AuNPs, all formulations precipitated but one, and it was not included in Table 1.

Finally, the optimized formula was obtained based on the data from Design Expert. Optimized formulations for AA-AuNPs and PH-AuNPs were achieved by the addition of 500 µL of plant extract to 10 mL of $HAuCl_4.3H_2O$ (1M) at pH 4. To synthesize MN-AuNPs, 500 µL of plant extract was added to 10 mL of $HAuCl_4.3H_2O$ (2 M) at pH 4. The reaction mixtures were heated in a water bath at 60 °C until the reaction started (the color of the $AuCl_4$ solution changed to deep purple). Table 2 shows the results of PS, ZP, and PDI for the optimized formulation of each extract.

Table 1. PS, PDI, and ZP of examined formulations of plant AuNPs. All formulations for PH-AuNPs precipitated, so data were not included.

Plant AuNPs	Variables	Volume of extract (mL)			Concentration of HAuCl4 (mM)			pH			Time (min)		
		0.5	**1**	**2**	**1**	**2**	**4**	**4**	**7**	**8**	**10**	**50**	**100**
MN-AuNPs	**PS (nm)**	75.1	112.9	118.6	133.6	63.2	109.7	84.8	104.1	117.7	67.1	108.9	130.5
	ZP (mV)	-3.8	-10.5	-10.0	-8.5	-6.8	-5.7	-8.4	-5.3	-10.6	-9.2	-7.7	-7.4
	PDI	0.4	0.6	0.5	0.4	0.5	0.6	0.6	0.5	0.4	0.6	0.5	0.5
Plant AuNPs	**Variables**	**Volume of extract (mL)**			**Concentration of HAuCl4 (mM)**			**pH**			**Time (min)**		
		0.5	**2**	**4**	**1**	**2**	**4**	**4**	**7**	**8**	**10**	**50**	**100**
AA-AuNPs	**PS (nm)**	138.4	127.8	128.5	116.0	122.8	155.9	94.2	143.4	157.2	97.1	167.0	130.6
	ZP (mV)	-4.9	-4.5	-5.4	-3.9	-5.9	-4.8	-3.3	-6.6	-4.8	-5.4	-5.6	-3.7
	PDI	0.4	0.3	0.3	0.4	0.3	0.3	0.4	0.3	0.3	0.4	0.3	0.3

PS, Particle size; PDI, polydispersity index; ZP, zeta potential; AuNPs, gold nanoparticles; AA, *Artemisia absinthium;* MN, *Morus nigra;* PH, *Peganum harmala.*

Table 2. DLS analysis results of optimized formulations.

Plant AuNPs	Volume of extract AuNPs (µL)	Concentration of HAuCl4 (mM)	pH	PS (nm)	PDI	ZP (mV)
AA-AuNPs	500	1	4	65.18	0.401	-8.0
MN-AuNPs	500	2	4	69.13	0.123	-26.6
PH-AuNPs	500	1	4	217.80	0.291	-19.8

PS, Particle size; PDI, polydispersity index; ZP, zeta potential; AuNPs, gold nanoparticles; AA, *Artemisia absinthium;* MN, *Morus nigra;* PH, *Peganum harmala.*

UV-Vis spectroscopy

Ultraviolet-visible spectroscopy was used to determine the formation and stability of AuNPs (31). The formation of Au ions in the reaction mixture was visualized by changes in the color. In addition, the maximum peaks in the visible region were detected at 536.12, 546.93, and 553.13 nm for AA-AuNPs, MN-AuNPs, and PH-AuNPs, respectively, which corresponded to the intensity of surface plasmon resonance (SPR) bands.

FT-IR spectroscopic analysis

FT-IR spectroscopy was used to analyze the newly formed functional groups of active biomolecules. The FT-IR spectra of AA aerial parts, MN fruit, PH seed extracts, and their AuNPs are shown in Fig. 1. The chromatogram of AA extract exhibited major vibration stretches at 3365.17, 2927.41, 1633.41, 1402, 1261.22, 1066.44, and 616.145 cm^{-1}. The major peaks of MN extract were identified at 3398.92, 2925.48, 1725.98, 1623.77, 1420.23, 1260.25, 1053.91, and 630.61 cm^{-1}. PH extract showed absorbance at 3361.07, 2932.23, 1781.9, 1630.52, 1405.85, 1051.98, and 616.14 cm^{-1}. Major vibration stretches were similarly observed on synthesized AA-AuNPs at 3369.03, 2931.27, 1785.76, 1629.55, 1416.46, 1071.26 cm^{-1}. MN-AuNPs peaks were observed at 3387.35, 2924.52, 1731.76, 1644.02, 1419.35, 1055.84, and 590.11 cm^{-1}, and PH-AuNPs absorbance bands were seen at 3369.03, 2931.27, 1785.76, 1629.55, 1416.46, 1071.26, and 617.11 cm^{-1}.

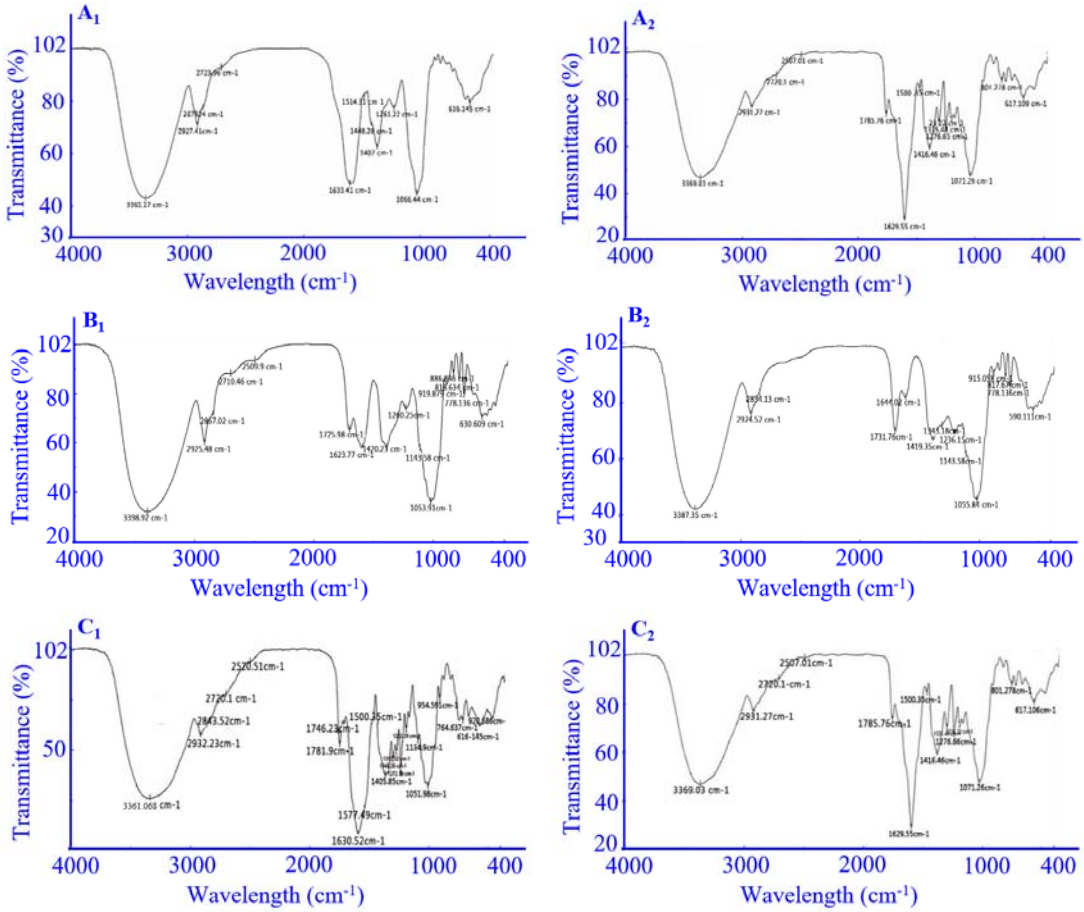

Fig. 1. Fourier-transform infrared spectra of plant extracts and synthesized AuNPs. (A_1) AA extract, (A_2) AA-AuNPs, (B_1) MN extract, (B_2) MN-AuNPs, (C_1) PH extract, (C_2), PH-AuNPs. AuNPs, Gold nanoparticles; AA, *Artemisia absinthium;* MN, *Morus nigra;* PH, *Peganum harmala*.

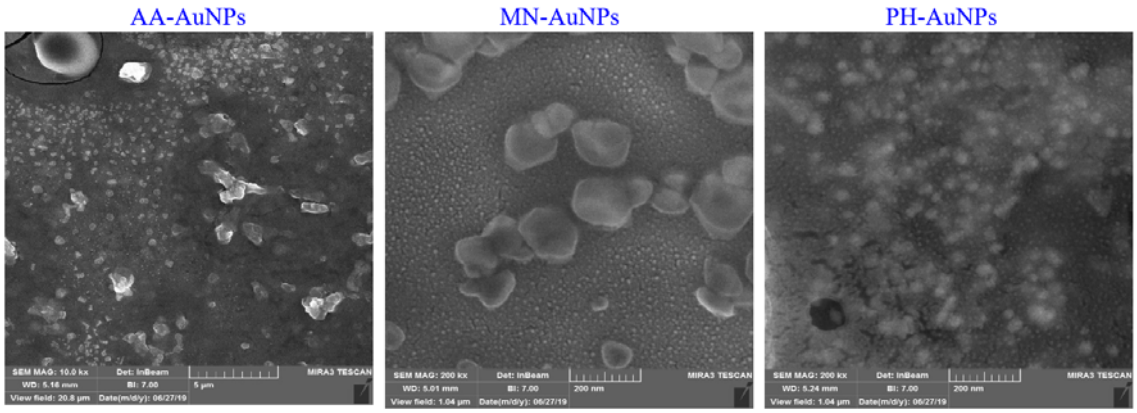

Fig. 2. Typical SEM images of AuNPs formed by plant extracts of (A) AA-AuNPs, (B) MN-AuNPs, and (C) PH-AuNPs. AuNPs, Gold nanoparticles; AA, *Artemisia absinthium;* MN, *Morus nigra;* PH, *Peganum harmala*; SEM, scanning electron microscope.

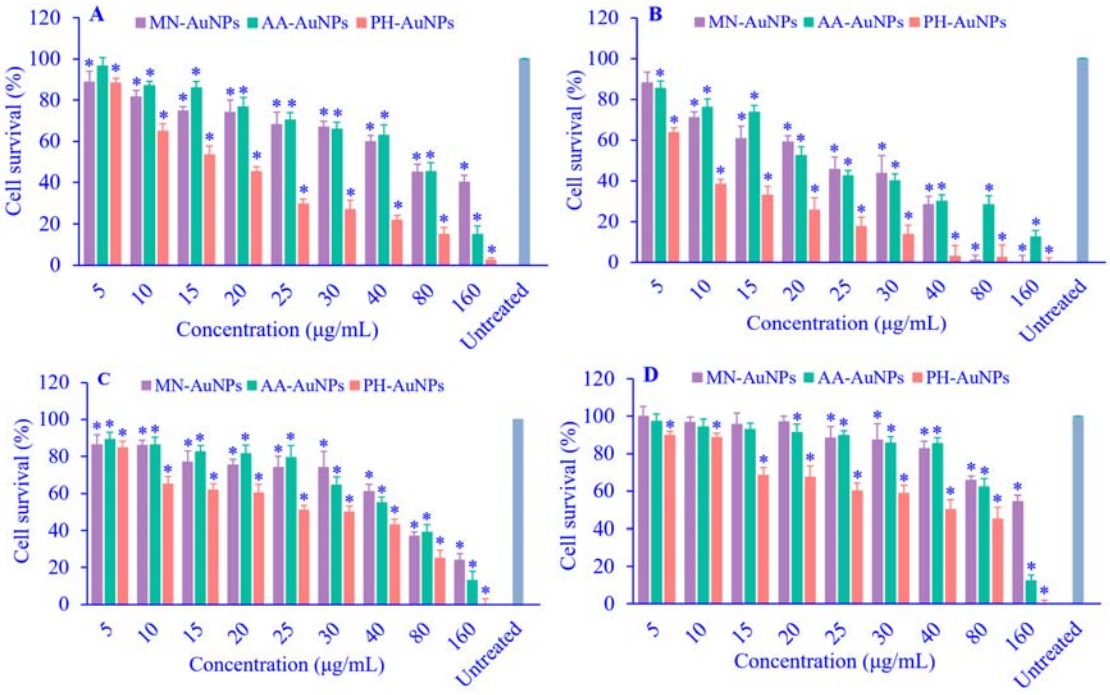

Fig. 3. *In vitro* cell cytotoxicity of different concentrations of AA-AuNPs, MN-AuNPs, and PH-AuNPs against (A) HT-29, (B) HeLa, (C) OVCAR3, and (D) MCF-7 cell lines. Untreated cells were used as the negative control. Data were expressed as mean ± SD, n = 3. $^{*}P < 0.05$ indicates a significant difference in comparison to untreated cells. AuNPs, Gold nanoparticles; AA, *Artemisia absinthium;* MN, *Morus nigra;* PH, *Peganum harmala.*

FE-SEM analysis

The FE-SEM image (Fig. 2) revealed that AA-AuNPs, MN-AuNPs, and PH-AuNPs were around 10-50 nm and mostly in hexagonal or spherical shape, which were smaller in size in comparison to the DLS results.

In vitro cytotoxic assay

The MTT-based colorimetric assay was applied to evaluate the cytotoxic effect of used plant-based AuNPs. AA-AuNPs, MN-AuNPs, and PH-AuNPs were shown to be cytotoxic against HT-29, HeLa, OVCAR3, and MCF-7 cell lines in a dose-dependent manner.

The viability of treated cells was significantly lower compared to control cells (untreated cells with 100% viability) (Fig. 3). The AA-AuNPs and MN-AuNPs showed lower toxicity, whereas the PH-AuNPs were more cytotoxic against cancer cells.

Applied cell lines showed different cytotoxic behaviors toward plant NPs. For example, human cervical epithelial carcinoma, HeLa ($IC_{50} \leq 31.5$ µg/mL) exhibited maximum sensitivity to 3 types of plant-AuNPs (Fig. 3). Moreover, among different plant extracts, PH-AuNPs were the most cytotoxic NPs against all tested cell lines, especially HeLa cells ($IC_{50} \leq 9.15$ µg/mL) (Fig. 3).

Flow cytometry assay

Plant NPs mostly showed their cytotoxic activity *via* the induction of apoptosis in a concentration-dependent manner. According to flow cytometry results, PH-AuNPs were the most cytotoxic compound against all tested cell lines at their IC_{50} concentration, followed by MN-AuNPs and AA-AuNPs. In addition, the percentage of early/late apoptotic and necrotic cells induced by PH-AuNPs were significantly different from others ($P < 0.05$) (Fig. 4).

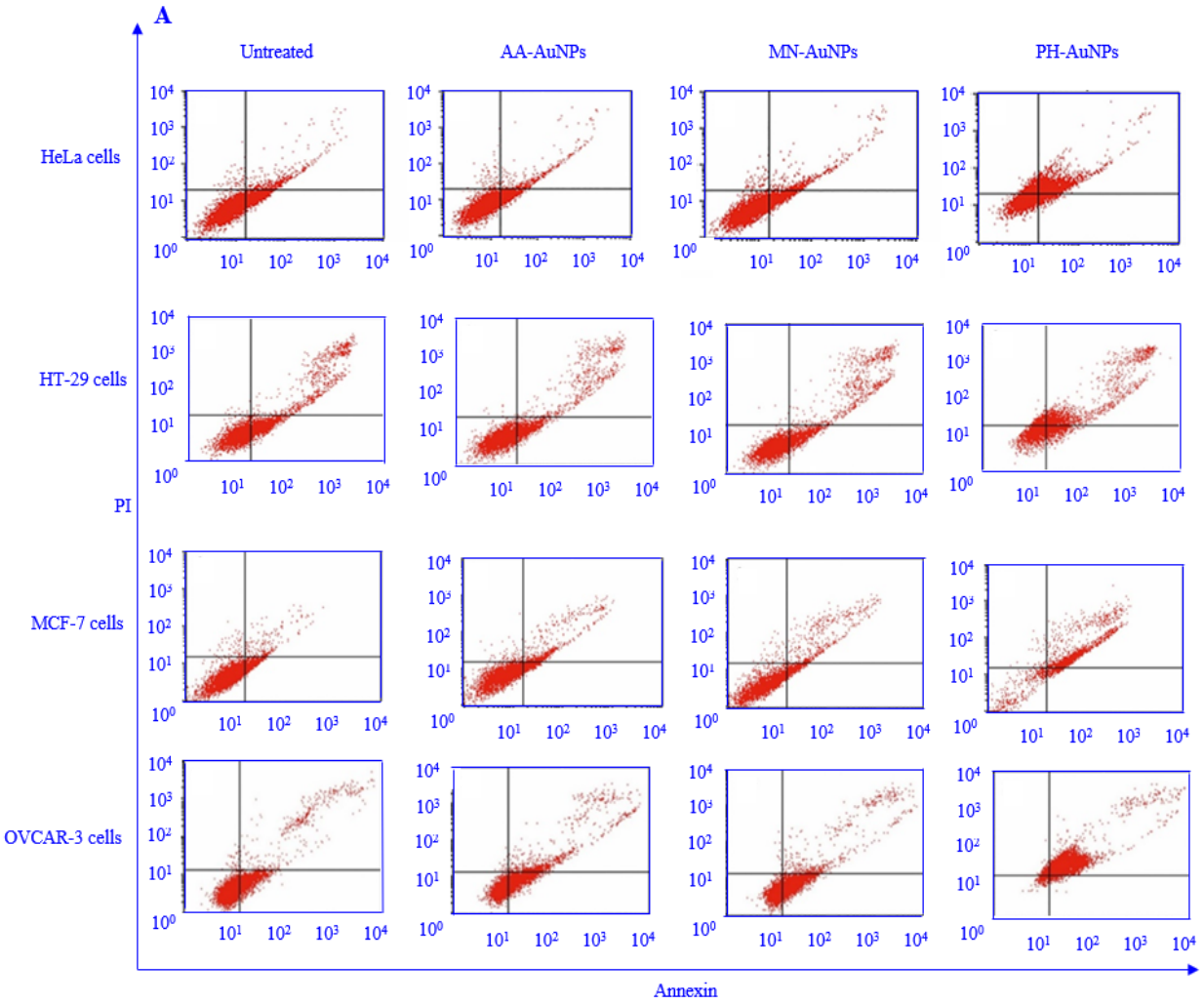

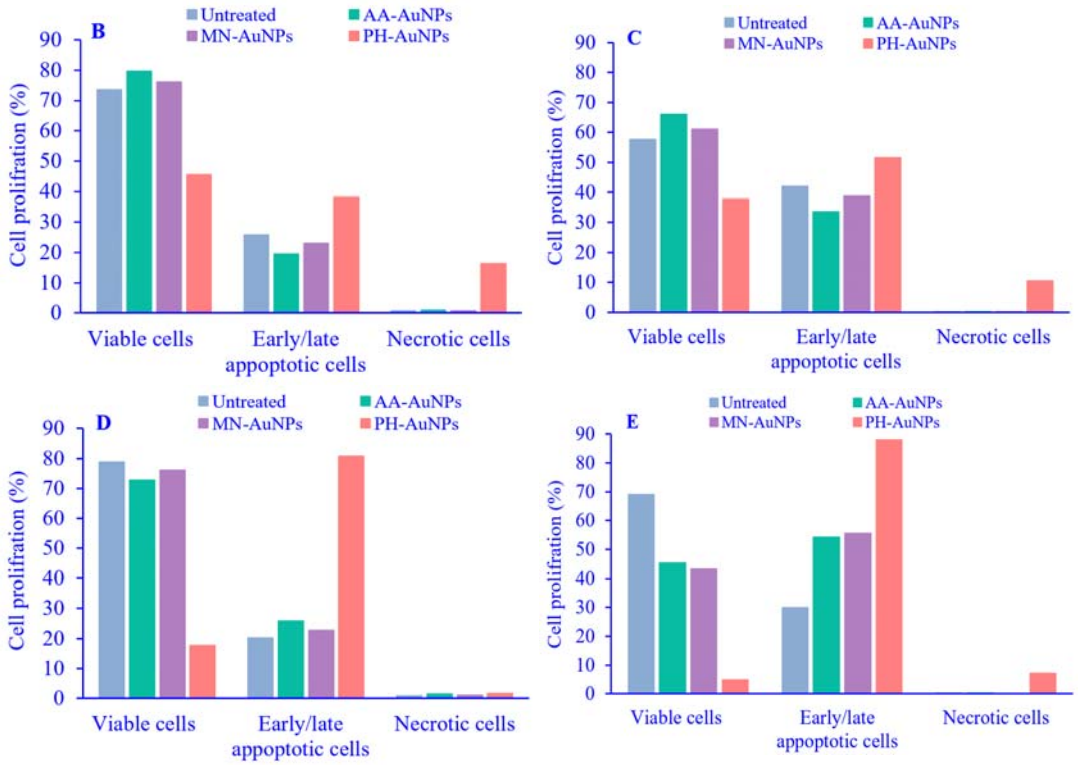

Fig. 4. Analysis of cell death mechanism by flow cytometry. HeLa, MCF-7, HT-29, and OVCAR-3 cells were treated with IC_{50} concentrations of plant-AuNPs for 24 h and then stained with Annexin V/PI. Non-treated cells were considered the negative control. (A) Annexin V/PI double-staining assay. HeLa cells were treated with AA-AuNPs, MN-AuNPs, and PH-AuNPs at the concentrations of 21.16, 23.37, and 7.69 µg/mL, respectively. HT-29 cells were treated with AA-AuNPs, MN-AuNPs, and PH-AuNPs at the concentrations of 71.24, 66.36, and 16.66 µg/mL, respectively. MCF-7 cells were treated with AA-AuNPs, MN-AuNPs, and PH-AuNPs at the concentrations of 99.72, 191.85, and 40 µg/mL, respectively. OVCAR3 cells were treated with AA-AuNPs, MN-AuNPs, and PH-AuNPs at the concentrations of 45, 58.33, and 30 µg/mL, respectively; cell proliferation in (B) HeLa, (C) HT-29, (D) MCF-7, and (E) OVCAR3 cell lines. Graphs B-E were derived from the flow cytometry results read once. AuNPs, Gold nanoparticles; AA, *Artemisia absinthium;* MN, *Morus nigra;* PH, *Peganum harmala.*

DISCUSSION

One of the interesting applications of plant extracts is their use in preparing synthetic metallic NPs. Using plant extracts is affordable, simple, fast, and, more importantly, environmental-friendly. The objective of this research was to create 3 distinct types of AuNPs utilizing plant extracts derived from the aerial parts of AA, the fruits of MN, and the seeds of PH.

Nowadays, the rate and the yield of reactions applied in the production of green NPs are comparable to chemical methods (30). The reaction rate, PS, and morphology depend on the plant type and its extract concentration, the concentration of the metal salt, the pH, temperature, and contact time (25). Many bio-reducing agents could be used to produce NPs. Amongst them, the use of plant extracts in the preparation of NPs is more advantageous over other expensive methodologies because plants are sustainable, renewable, and easily available and also safe to handle and process in the fabrication of NPs (31). In recent years, many plants used for this purpose have shown promising results (36,37). Many studies have shown that plants, including AA, MN, and PH, have cytotoxic effects; however, this effect has not been reported for AuNPs prepared from these plants (19,38,39). The extract of PH seeds, including harmaline, showed considerable cytotoxicity on cancer cell lines such as B19, B65, and PC12, while it had very low toxicity on normal cells (40). In addition, the anti-angiogenesis and anti-growth effects of

AA on breast cancer cells have been reported (41). Moreover, previous studies have documented that MN showed anticancer effects *via* inducing apoptotic cell death on HT-29, MCF-7, and HeLa cell lines (42-44). Considering the findings, *AA*, *MN*, and *PH* were selected for the biosynthesis of AuNPs due to their considerable cytotoxic effects. Taken together, 3 different AuNPs were prepared using plant extracts and then characterized. The FT-IR spectra showed that biomolecules were involved in the formation of plant-AuNPs by the reduction process, confirmed by the shifting of the peaks. Bands in the range of 3500-3000 cm^{-1} represented NH and OH stretching. Peaks at 2931, 2929, and 2924 cm^{-1} could be attributed to $-CH_2$ asymmetric stretching for the plant-AuNPs. The peaks ranging between 1070 and 1010 cm^{-1} in the spectral analysis were assigned to C-O and C-H chemical bonds. The SPR results were indicative of the formation of poly dispersed AuNPs (32-35). FE-SEM analysis revealed that the size of the NPs was smaller compared to DLS results. Ahmad *et al*. stated that the size differences between FE-SEM and DLS measurements could be explained by the fact that DLS measures the hydrodynamic radius of NPs in aqueous medium, which includes the metallic cores and any biological molecules attached to or adsorbed on the surfaces of particles (45). The biochemical compounds of the plant extracts influenced the hydrodynamic diameters of the synthesized plant AuNPs, which was indicated by DLS analysis. The real mechanism behind the formation of different-sized NPs is unclear (46,47). As previously reported, the polydisperse nature of AuNPs might be due to the involvement of various reducing compounds that exist in the plant extract (47-50).

Consistent with the current results, other studies have also shown the cytotoxic effect of biologically synthesized plant-AuNPs (51,52). AgNPs from plant extracts could also show the same cytotoxic results (53). The present results also demonstrated the difference of plant NPs on cell lines such as HeLa cells. One study has also shown that HeLa cells were more sensitive to plant-based AgNPs (54). Moreover, the most significant cytotoxic effects were exhibited by PH-AuNPs on all tested cell lines, especially on HeLa cells. Therefore, PH-AuNPs might be a considerable cytotoxic agent against cervical malignancies. Other green-based AuNPs have also been shown to be cytotoxic to cancer cell lines such as MCF-7 and HeLa, probably by promoting cell cycle arrest and apoptosis (55,56). In particular, using plant-based AuNPs looks like a promising approach for killing ovarian cancer cells, since ovarian cancer cells, such as PA-1, SW-626, SK-OV-3, and HeLa cells in our study, showed high sensitivity to plant-based AuNPs (57). Interestingly, green biologically synthesized AuNPs might have better anti-tumor activities than chemically synthesized ones, as one study showed that AuNPs of *Ocimum tenuiflorum* were more toxic to cancer cell growth (HeLa and MCF-7 cell lines) compared to AuNPs capped with citrate (56). The cytotoxic effect of plant-based NPs can also be attributed to the bioactive compounds, including alkaloids, flavonoids, and phenols in the plants, which lead to cell cycle arrest, cell death, and apoptosis in cancer cells (58-60).

Many mechanisms have been discussed for the cytotoxic effects of AuNPs capped by plant extracts (55). Oxidative stress and the generation of reactive species are found to be the most accepted mechanisms involved in the *in vitro* cytotoxic effects of NPs against cancer cell lines, in particular HeLa cells. The cytotoxic activity may also be due to the direct action of Au ions released from NPs, which may interact with mitochondrial functions, initiating stress pathways and apoptosis (48).

CONCLUSION

The current study successfully developed an eco-friendly procedure and synthesized AuNPs with the aid of different plant extracts, including AA aerial parts, MN fruits, and PH seeds. The evaluation of the NPs revealed that they were biosynthesized efficiently. FT-IR characterization demonstrated the major vibration stretches by the reduction process. The FE-SEM images indicated that the AuNPs ranged in size from 10-50 nm and were mostly hexagonal or spherical, after green synthesis. In this study, results exhibited a dose-dependent

cytotoxic activity of NPs against cancer cell lines, namely HeLa, HT-29, MCF-7, and OVCAR3 *via* an apoptotic mechanism. It was found that PH-AuNPs were the most potent NPs against all tested cancer cells, especially HeLa cells. More studies should be done to find out the active ingredient in the plants, such as PH, which makes the NPs cytotoxic. The ability of plants to act as capping and reducing agents can be potentially exploited to formulate metallic NPs since they are inexpensive, easily accessible, and renewable resources. Additionally, due to their considerable cytotoxicity, their application as a cancer treatment option is a promising approach that warrants further investigation.

Acknowledgements

This research was financially supported by the Research Deputy of Isfahan University of Medical Sciences as a Pharm. D thesis (Grant No. 397133).

Conflicts of interest statement

All authors declared no conflict of interest in this study.

Authors' contributions

M. Mirian, F. Rahimi, and H. Sadeghi-aliabadi designed the research; A. Banizaman and S. Sepahi performed the research; M. Sadeghi-aliabadi and M. Rezazadeh analyzed the data and revised the paper; M. Mirian and H. Sadeghi-aliabadi drafted, reviewed, and revised the manuscript. All authors read and confirmed the final version of the manuscript.

REFERENCES

1. Iravani S. Green synthesis of metal nanoparticles using plants. Green Chem. 2011;13(10):2638-2850. DOI: 10.1039/C1GC15386B.
2. Shamaeizadeh N, Varshosaz J, Mirian M, Aliomrani M. Glutathione targeted tragacanthic acid-chitosan as a non-viral vector for brain delivery of miRNA-219a-5P:*an in vitro/in vivo* study. Int J Biol Macromol. 2022;200:543-556. DOI: 10.1016/j.ijbiomac.2022.01.100.
3. Botha TL, James TE, Wepener V. Comparative aquatic toxicity of gold nanoparticles and ionic gold using a species sensitivity distribution approach. J Nanomater. 2015;2015:1-16. DOI: 10.1155/2015/986902.
4. Botha TL, Elemike EE, Horn S, Onwudiwe DC, Giesy JP, Wepener V. Cytotoxicity of Ag, Au and Ag-Au bimetallic nanoparticles prepared using golden rod (Solidago canadensis) plant extract. Sci Rep. 2019;9:4169,1-8. DOI: 10.1038/s41598-019-40816-y.
5. Zhang XF, Liu ZG, Shen W, Gurunathan S. Silver nanoparticles: synthesis, characterization, properties, applications, and therapeutic approaches. Int J Mol Sci. 2016;17(9):1534,1-34. DOI: 10.3390/ijms17091534.
6. Mirian M, Khanahmad H, Darzi L, Salehi M, Sadeghi-Aliabadi H. Oligonucleotide aptamers: potential novel molecules against viral hepatitis. Res Pharm Sci. 2017;12(2):88-98. DOI: 10.4103/1735-5362.202447.
7. Lee J, Chatterjee DK, Lee MH, Krishnan S. Gold nanoparticles in breast cancer treatment: promise and potential pitfalls. Cancer Lett. 2014;347(1):46-53. DOI: 10.1016/j.canlet.2014.02.006.
8. Lewinski N, Colvin V, Drezek R. Cytotoxicity of nanoparticles. Small. 2008;4(1):26-49. DOI: 10.1002/smll.200700595.
9. Thwala M, Musee N, Sikhwivhilu L, Wepener V. The oxidative toxicity of Ag and ZnO nanoparticles towards the aquatic plant Spirodela punctuta and the role of testing media parameters. Environ Sci Process Impacts. 2013;15(10):1830-1843. DOI: 10.1039/C3EM00235G.
10. Aboyewa JA, Sibuyi NR, Meyer M, Oguntibeju OO. Green synthesis of metallic nanoparticles using some selected medicinal plants from southern Africa and their biological applications. Plants. 2021;10(9):1929,1-24. DOI: 10.3390/plants10091929.
11. Bawazeer S, Rauf A, Shah SUA, Shawky AM, Al-Awthan YS, Bahattab OS, *et al*. Green synthesis of silver nanoparticles using *Tropaeolum majus*: phytochemical screening and antibacterial studies. Green Process Synth. 2021;10(1):85-94. DOI: 10.1515/gps-2021-0003.
12. Siddiqi KS, Husen A, Rao RA. A review on biosynthesis of silver nanoparticles and their biocidal properties. J Nanobiotechnology. 2018;16(1):14,1-28. DOI: 10.1186/s12951-018-0334-5.
13. Iranshahy M, Bazzaz SF, Haririzadeh G, Abootorabi BZ, Mohamadi AM, Khashyarmanesh Z. Chemical composition and antibacterial properties of *Peganum harmala L*. Avicenna J Phytomed. 2019;9(6):530-539. DOI: 10.22038/AJP.2019.13382.
14. Asadzadeh R, Abbasi N, Bahmani M. Extraction and identification of chemical compounds of *Peganum harmala L.* seed essential oil by HS-SPME and GC-MS methods. Tradit Integr Med. 2021;6(3):229-235. DOI: 10.18502/tim.v6i3.7310.
15. Farouk L, Laroubi A, Aboufatima R, Benharref A, Chait A. Evaluation of the analgesic effect of alkaloid extract of *Peganum harmala L.*: possible mechanisms involved. J Ethnopharmacol. 2008;115(3):449-454. DOI: 10.1016/j.jep.2007.10.014.

16. Panahi Y, Saadat A, Seifi M, Rajaee M, Butler AE, Sahebkar A. Effects of Spinal-Z in patients with gastroesophageal cancer. J Pharmacopuncture. 2018;21(1):26-34.
DOI: 10.3831/KPI.2018.21.004.
17. Msaada K, Salem N, Bachrouch O, Bousselmi S, Tammar S, Alfaify A, *et al*. Chemical composition and antioxidant and antimicrobial activities of wormwood (*Artemisia absinthium L.*) essential oils and phenolics. J Chem. 2015;2015(1):804658,1-12.
DOI: 10.1155/2015/804658.
18. Basta A, Tzakou O, Couladis M, Pavlović M. Chemical composition of *Artemisia absinthium L.* from Greece. J Essent Oil Res. 2007;19(4):316-318.
DOI: 10.1080/10412905.2007.9699291.
19. Shafi G, Hasan TN, Syed NA, Al-Hazzani AA, Alshatwi AA, Jyothi A, *et al*. *Artemisia absinthium* (AA): a novel potential complementary and alternative medicine for breast cancer. Mol Biol Rep. 2012;39(7):7373-7379.
DOI: 10.1007/s11033-012-1569-0.
20. Kostic DA, Dimitrijevic DS, Mitic SS, Mitic MN, Stojanovic GS, Zivanovic AV. Phenolic contents and antioxidant activity of fruit extracts of *Murus nigra L* (Muraceae) from southeast Serbia. Trop J Pharm Res. 2013; 12(1):105-110.
DOI: 10.4314/tjpr.v12i1.17.
21. Ercisli S, Orhan E. Chemical composition of white (*Morus alba*), red (*Morus rubra*) and black (*Morus nigra*) mulberry fruits. Food Chem. 2007;103(4):1380-1384.
DOI: 10.1016/j.foodchem.2006.10.054.
22. Imran M, Khan H, Shah M, Khan R, Khan F. Chemical composition and antioxidant activity of certain Morus species. J Zhejiang Univ Sci B. 2010;11(12):973-980.
DOI: 10.1631/jzus.B1000173.
23. Keskin C, Atalar MN, Baran MF, Baran A. Environmentally friendly rapid synthesis of gold nanoparticles from *Artemisia absinthium* plant extract and application of antimicrobial activities. J Inst Sci Technol. 2021;11(1):365-367.
DOI: 10.21597/jist.779169.
24. Moustafa NE, Alomari AA. Green synthesis and bactericidal activities of isotropic and anisotropic spherical gold nanoparticles produced using *Peganum harmala L.* leaf and seed extracts. Biotechnol Appl Biochem. 2019;66(4):664-672.
DOI: 10.1002/bab.1782.
25. Klahs, PC, McMurchie EK, Nikkel JJ, Clark LG. A maceration technique for soft plant tissue without hazardous chemicals. Appl Plant Sci. 2023;11(5):e11543,1-10.
DOI: 10.1002/aps3.11543.
26. Ahmad A, Syed F, Shah A, Khan Z, Tahir K, Khan AU, *et al*. Silver and gold nanoparticles from Sargentodoxa cuneata: synthesis, characterization and antileishmanial activity. RSC Adv. 2015;5(90):73793-73806.
DOI: 10.1039/CSRA13206A.
27. Velusamy P, Kumar GV, Jeyanthi V, Das J, Pachaiappan R. Bio-inspired green nanoparticles: synthesis, mechanism, and antibacterial application. Toxicol Res. 2016;32(2):95-102.
DOI: 10.5487/TR.2016.32.2.095.
28. Hassanzadeh F, Sadeghi-Aliabadi H, Jafari E, Sharifzadeh A, Dana N. Synthesis and cytotoxic evaluation of some quinazolinone- 5-(4-chlorophenyl) 1, 3, 4-oxadiazole conjugates. Res Pharm Sci. 2019;14(5):408-413.
DOI: 10.4103/1735-5362.268201.
29. Kazemi Pilehrood M, Dilamian M, Mirian M, Sadeghi-Aliabadi H, Maleknia L, Nousiainen P, *et al*. Nanofibrous chitosan-polyethylene oxide engineered scaffolds: a comparative study between simulated structural characteristics and cells viability. Biomed Res Int. 2014;2014:438065,1-9.
DOI: 10.1155/2014/438065.
30. Noruzi M. Biosynthesis of gold nanoparticles using plant extracts. Bioprocess Biosyst Eng. 2015;38(1):1-14.
DOI: 10.1007/s00449-014-1251-0.
31. Premasudha P, Venkataramana M, Abirami M, Vanathi P, Krishna K, Rajendran R. Biological synthesis and characterization of silver nanoparticles using *Eclipta alba* leaf extract and evaluation of its cytotoxic and antimicrobial potential. Bull Mater Sci. 2015;38(4):965-973.
DOI: 10.1007/s12034-015-0945-5.
32. Aljabali AA, Akkam Y, Al Zoubi MS, Al-Batayneh KM, Al-Trad B, Abo Alrob O, *et al*. Synthesis of gold nanoparticles using leaf extract of *Ziziphus zizyphus* and their antimicrobial activity. Nanomaterials. 2018;8(3):174,1-15.
DOI: 10.3390/nano8030174.
33. Fazal S, Jayasree A, Sasidharan S, Koyakutty M, Nair SV, Menon D. Green synthesis of anisotropic gold nanoparticles for photothermal therapy of cancer. ACS Appl Mater Interfaces. 2014;6(11):8080-8089.
DOI: 10.1021/am500302t.
34. Kang JP, Kim YJ, Singh P, Huo Y, Soshnikova V, Markus J, *et al*. Biosynthesis of gold and silver chloride nanoparticles mediated by *Crataegus pinnatifida* fruit extract: *in vitro* study of anti-inflammatory activities. Artif Cells Nanomed Biotechnol. 2018;46(8):1530-1540.
DOI: 10.1080/21691401.2017.1376674.
35. Logeswari P, Silambarasan S, Abraham J. Synthesis of silver nanoparticles using plants extract and analysis of their antimicrobial property. J Saudi Chem Soc. 2015;19(3):311-317.
DOI: 10.1016/j.jscs.2012.04.007.
36. Nair HB, Sung B, Yadav VR, Kannappan R, Chaturvedi MM, Aggarwal BB. Delivery of anti-inflammatory nutraceuticals by nanoparticles for the prevention and treatment of cancer. Biochem Pharmacol. 2010;80(12):1833-1843.
DOI: 10.1016/j.bcp.2010.07.021.
37. Gangwar RK, Dhumale VA, Kumari D, Nakate UT, Gosavi S, Sharma RB, *et al*. Conjugation of curcumin with PVP capped gold nanoparticles for improving bioavailability. Mater Sci Eng C. 2012;32(8):2659-2663.
DOI: 10.1016/j.msec.2012.07.022.

38. Seyed Hassan Tehrani S, Hashemi Sheikh Shabani S, Tahmasebi Enferadi S, Rabiei Z. Growth inhibitory impact of *Peganum harmala L*. on two breast cancer cell lines. Iran J Biotechnol. 2014;12(1):8-14. DOI: 10.5812/ijb.18562.
39. de Freitas MM, Fontes PR, Souza PM, Fagg CW, Guerra ENS, de Medeiros Nóbrega YK, *et al*. Extracts of *Morus nigra L*. leaves standardized in chlorogenic acid, rutin, and isoquercitrin: tyrosinase inhibition and cytotoxicity. PLoS One. 2016;11(9) e0163130,1-24. DOI: 10.1371/journal.pone.0163130.
40. Mohammad MH, Kadhum MEH, Abdul-Muniam Ali Z. Cytotoxic effect of *Peganum harmala L*. extract and induction of apoptosis on cancerous cell line. Iraqi J Cancer Med Genet. 2010;3(1):11-16. DOI: 10.29409/ijcmg.v3i1.21.
41. Emami SA, Vahdati-Mashhadian N, Vosough R, Oghazian MB. The anticancer activity of five species of Artemisia on Hep2 and HepG2 cell lines. Pharmacol Online. 2009;3:327-339.
42. Qadir MI, Ali M, Ibrahim Z. Anti-cancer activity of *Morus nigra* leaves extract. Bangladesh J Pharmacol. 2014;9(4):496-497. DOI: 10.3329/bjp.v9i4.19783.
43. Ahmed A, Ali M, El-Kholie E, El-Garawani I, Sherif N. Anticancer activity of *Morus nigra* on human breast cancer cell line (MCF-7): the role of fresh and dry fruit extracts. J Biosci Appl Res. 2016;6(2):352-361. DOI: 10.21608/JBAAR.2016.108382.
44. Çakıroğlu E, Uysal T, Çalıbaşı Koçal G, Aygenli F, Baran G, Baskın Y. The role of *Morus nigra* extract and its active compounds as drug candidate on human colorectal adenocarcinoma cell line HT-29. Int J Clin Oncol Cancer Res. 2017;2(1):10-14. DOI: 10.11648/j.ijcocr.20170201.13.
45. Ahmad T, Wani IA, Manzoor N, Ahmed J, Asiri AM. Biosynthesis, structural characterization, and antimicrobial activity of gold and silver nanoparticles. Colloids Surf B Biointerfaces. 2013;107:227-234. DOI: 10.1016/j.colsurfb.2013.02.004.
46. Patil MP, Jin X, Simeon NC, Palma J, Kim D, Ngabire D, *et al*. Anticancer activity of *Sasa borealis* leaf extract-mediated gold nanoparticles. Artif Cells Nanomed Biotechnol. 2018;46(1):82-88. DOI: 10.1080/21691401.2017.1293675.
47. Roy S, Das TK, Maiti GP, Basu U. Microbial biosynthesis of non-toxic gold nanoparticles. Mater Sci Eng B. 2016;203:41-51. DOI: 10.1016/j.mseb.2015.10.008.
48. Benelli G. Green synthesized nanoparticles in the fight against mosquito-borne diseases and cancer-a brief review. Enzyme Microb Technol. 2016;95:58-68. DOI: 10.1016/j.enzmictec.2016.08.022.
49. Rajan A, Rajan AR, Philip D. *Elettaria cardamomum* seed mediated rapid synthesis of gold nanoparticles and its biological activities. OpenNano. 2016;2(C): 1-8. DOI: 10.1016/j.onano.2016.11.002.
50. Wang C, Mathiyalagan R, Kim YJ, Castro-Aceituno V, Singh P, Ahn S, *et al*. Rapid green synthesis of silver and gold nanoparticles using *Dendropanax morbifera* leaf extract and their anticancer activities. Int J Nanomedicine. 2016;11:3691-3701. DOI: 10.2147/IJN.S97181.
51. Vijayakumar S, Ganesan S. *In vitro* cytotoxicity assay on gold nanoparticles with different stabilizing agents. J Nanomater. 2012;2012:1-8. DOI: 10.1155/2012/734398.
52. Zhu Y, Liao L. Applications of nanoparticles for anticancer drug delivery: a review. J Nanosci Nanotechnol. 2015;15(7):4753-4773. DOI: 10.1166/jnn.2015.10298.
53. Kumari R, Saini AK, Kumar A, Saini RV. Apoptosis induction in lung and prostate cancer cells through silver nanoparticles synthesized from *Pinus roxburghii* bioactive fraction. J Biol Inorg Chem. 2020;25(1):23-37. DOI: 10.1007/s00775-019-01729-3.
54. De Matteis V, Rizzello L, Ingrosso C, Liatsi-Douvitsa E, De Giorgi ML, De Matteis G, *et al*. Cultivar-dependent anticancer and antibacterial properties of silver nanoparticles synthesized using leaves of different *Olea europaea* trees. Nanomaterials. 2019;9(11):1544,1-24. DOI: 10.3390/nano9111544.
55. Balashanmugam P, Durai P, Balakumaran MD, Kalaichelvan PT. Phytosynthesized gold nanoparticles from *C. roxburghii* DC. leaf and their toxic effects on normal and cancer cell lines. J Photochem Photobiol B Biol. 2016;165: 163-173. DOI: 10.1016/j.jphotobiol.2016.10.013.
56. Virmani I, Sasi C, Priyadarshini E, Kumar R, Sharma SK, Singh GP, *et al*. Comparative anticancer potential of biologically and chemically synthesized gold nanoparticles. J Clust Sci. 2020;31(4):867-876. DOI: 10.1007/s10876-019-01695-5.
57. Chen J, Li Y, Fang G, Cao Z, Shang Y, Alfarraj S, *et al*. Green synthesis, characterization, cytotoxicity, antioxidant, and anti-human ovarian cancer activities of *Curcumae kwangsiensis* leaf aqueous extract green-synthesized gold nanoparticles. Arab J Chem. 2021;14(3):103000,1-9. DOI: 10.1016/j.arabjc.2021.103000.
58. Yadegarynia S, Pham A, Ng A, Nguyen D, Lialiutska T, Bortolazzo A, *et al*. Profiling flavonoid cytotoxicity in human breast cancer cell lines: determination of structure-function relationships. Nat Prod Commun. 2012;7(10):1295-1304. PMID: 23156993.
59. Bouyahya A, Omari NE, Bakrim S, Hachlafi NE, Balahbib A, Wilairatana P, *et al*. Advances in dietary phenolic compounds to improve chemosensitivity of anticancer drugs. Cancers. 2022;14(19):4573,1-20. DOI: 10.3390/cancers14194573.
60. Khan H, Alam W, Alsharif KF, Aschner M, Pervez S, Saso L. Alkaloids and colon cancer: molecular mechanisms and therapeutic implications for cell cycle arrest. Molecules. 2022;27(3):920,1-26. DOI: 10.3390/molecules27030920.